Cost-Efficient Power Orchestration in Heterogeneous EV-Integrated VPPs: A Peak Demand Repair Scheme

Ahmed F. Selim
EE Department
King Fahd Univ. of
Petroleum & Minerals
Dhahran, Saudi Arabia
g200992570@kfupm.edu.sa

Mohammed A. Abido, S.M.IEEE
EE Department
King Fahd Univ. of
Petroleum & Minerals
Dhahran, Saudi Arabia
m.abido@kfupm.edu.sa

Ali T. Al-Awami, S.M.IEEE
EE Department
King Fahd Univ. of
Petroleum & Minerals
Dhahran, Saudi Arabia
aliawami@kfupm.edu.sa

***Abstract*—Vehicle-to-Grid (V2G) technology enables Electric Vehicles (EVs) to function as Virtual Power Plants (VPPs) which provide essential grid support services. The operational process becomes highly difficult because the system needs to handle electric vehicles which have different battery capabilities while it tries to achieve three different goals. This investigation resolves the major "horizon effect" problem which occurs in real-time rolling-horizon optimization because short-term economic planning cannot prevent peak charges from occurring within the monthly period. The research demonstrates that standard heuristic methods which use V2G arbitrage for their operations cannot handle extended periods of load density because they result in critical constraint breaches which create additional demand expenses. The research presents a Peak-Repair Particle Swarm Optimization (PR-PSO) algorithm which uses Laxity-Based Pruning for its operation. The PR-PSO system successfully controlled total peak demand during extreme usage patterns which were tested with 10 commercial EV models throughout a 30-day billing cycle using 11-run Monte Carlo statistical analysis. The proposed mechanism established physical search boundaries through its conversion of soft economic penalties which resulted in 100% session completion and a Net Total Cost decrease of approximately 40% compared to standard rolling-horizon and uncoordinated benchmarks.**

***Index Terms*—Electric Vehicles (EVs), Vehicle-to-Grid (V2G), Virtual Power Plant (VPP), Particle Swarm Optimization (PSO), Heterogeneous Fleet, Demand Charge Management.**

I. Nomenclature

Symbol	Definition
Abbreviations	
VPP	Virtual Power Plant
DER	Distributed Energy Resource
EV	Electric Vehicle
V2G	Vehicle-to-Grid
PSO	Particle Swarm Optimization
PR-PSO	Peak-Repair PSO
MILP	Mixed-Integer Linear Programming
SoC	State of Charge
SoH	State of Health

Symbol	Definition
DoD	Depth of Discharge

Indices & Sets	
t, T	Time step index / Horizon
$n, \mathcal{N}$	Vehicle index / Set of vehicles

Parameters & Variables	
$r^n(t)$	Charging rate of vehicle n (kW)
C^n_{cap}	Battery capacity of vehicle n (kWh)
$p(t)$	ToU electricity price ($/kWh)
R_{demand}	Demand charge rate ($/kW-month)
P_{peak}	Max aggregate power (kW)
P^{hist}_{peak}	Historical peak power (kW)
C_{deg}	Battery degradation cost ($)
V^n_{bat}	Battery replacement cost ($/kWh)
N_{cyc}	Cycle life (cycles to failure)
r^{lax}_{min}	Laxity-based minimum power
γ^n	Reducible power margin

II. Introduction

The widespread adoption of electric transportation together with its global transition will create unpredictable energy demands which will stress the electrical grid system. The degree of stress on the grid system will depend on the actual power consumption that occurs. Real-world trials, such as the residential orchestration study in New Zealand, have confirmed that "fit-and-forget" or uncoordinated charging approaches lead to significant capacity constraints at the Low Voltage (LV) level. Along with this, the application of Vehicle-to-Grid (V2G) technology would make battery-operated vehicles not just consumers of power but also sources of storage in transit [5]. One of the major developments in this area has been the creation of Virtual Power Plants (VPPs) concept to synchronize and group these Distributed Energy Resources (DERs) effectively. However, the effective management of VPPs is still facing a massive challenge owing to the differing kinds of assets involved, unpredictable customer behavior, and the complexity in the representation of battery wear-off [1].

The management of VPPs has been the subject of various research papers applying different optimization methods. The studies based on standard linear programming processes mainly supply the most favorable schedules and hence, are a preferred choice. For instance, Muqbel et al. [19] demonstrated the efficacy of MILP for the optimal planning of distributed BESS in unbalanced distribution networks, though such planning models differ from real-time operation. Khezri et al. [12] refined V2G timing using a MILP while simultaneously considering calendar and cycle life of batteries. They proved that this demanding lifetime modeling is necessary for proper and realistic cost-benefit analysis. Rahman et al. [11] on the other hand, proposed stochastic optimization techniques for V2G-enabled VPPs participating in day-ahead and imbalance markets and highlighted the profitability of bidirectional charging.

MILP-based methods, despite their optimality, usually struggle with computational scalability. Moreover, when simulating real-time applications with rolling horizons they could under perform or provide sub-optimal solutions. Heuristic and meta-heuristic approaches have gained traction in this scope to address these limitations. Researchers have used Particle Swarm Optimization (PSO) and Genetic Algorithms (GA) to solve complex charging station operational challenges according to the study in reference [4], [17]. Wang et al. [20] introduced the Snow Ablation Optimizer (SAO) for VPP scheduling which decreases renewable energy curtailment while Saner et al. [21] studied heuristic approaches for modular fast-charging stations which effectively managed their hardware-specific operational restrictions. Joshua et al. [14] used GAs together with deep learning (DL) models to decrease waiting times at smart grid charging stations.

VPP systems now utilize recently developed machine learning (ML) and reinforcement learning (RL) techniques which scientists have incorporated into their control systems. Dong et al. [2] and Zheng et al. [1] proposed Multi-Agent Reinforcement Learning (MARL) for decentralized EV scheduling. They enabled agents to make autonomous decisions without a central coordinator. Other decentralized approaches, such as the proportional weight-based controller by Hossain et al. [22], effectively mitigate local voltage violations without central communication, though they may lack global visibility of peak charges. These works were further extended by Park and Moon [13] through developing a MARL approach with centralized training and decentralized execution. They specifically targeted the stochastic nature of EV arrivals. In addition, sophisticated forecasting models which incorporated LSTM and DL were applied to predict user behavior and renewable generation to support these control strategies. This is evident in the works of Rahman et al. [16] and Lilhore et al. [15].

A significant gap in the literature related to controlling the total peak demand charges still remains within these frameworks. Some studies such as [3] and [10] usually highlight frequency regulation or energy arbitrage but exclude demand charges and their monthly nature which may represent a considerable part of a commercial VPP's operating expenses. Similarly, adaptive strategies for opportunistic users [23] focus on maximizing charging station utilization but may inadvertently increase peak loads if not explicitly constrained. Algorithms that are optimized for a short horizon (e.g., 24 hours) might not take into account the single highest peak demand that sets the monthly penalty - a situation we refer to as "peak myopia." On the other hand, standard heuristics find it hard to maintain the strict aggregate limits over the large and diverse fleets [9].

This work addresses these gaps by:

1) Modeling a realistic Heterogeneous EV Fleet comprising of distinct commercial EV models, reflecting the diversity seen in modern charging datasets [7], [8].
2) Developing a modified formulation of the linearized model in [12], namely Peak-Repair PSO (PR-PSO), that embeds domain-specific constraints directly into the search process. It thus bridges the gap between heuristic flexibility and rigorous constraint satisfaction.
3) Benchmarking against dumb charging schemes like First-Come First Serve (FCFS) and Rolling-Horizon PSO. This benefits in demonstrating the superior handling of demand charges compared to traditional optimization methods.

III. Problem Formulation

A VPP at a commercial charging station equipped with bidirectional chargers is used to model the EV-integrated system. The charging rate $r^n(t)$ for each EV n from a heterogeneous fleet $\mathcal{N}$ is set at time t by a central controller to minimize operational costs over a billing period T.

A. Objective Function

The goal is to minimize the total cost which includes energy imports (charging/ discharging), demand charges, and battery degradation:

$$\min \left(\sum_{t=1}^{T} \left[C_{\text{energy}}(t) + C_{\text{deg}}(t) \right] \right) + C_{\text{demand}} \tag{1}$$

B. Cost Components

1) Energy and Demand: Time-of-Use (ToU) tariffs $p(t)$ affect the energy costs, while demand charges apply to the recorded maximum aggregate peak:

$$C_{\text{energy}}(t) = \sum_{n=1}^{N} r^n(t) \cdot \Delta t \cdot p(t) \tag{2}$$

$$C_{\text{demand}} = \max_{t \in T} \left(\sum_{n=1}^{N} r^n(t) \right) \cdot R_{\text{demand}} \tag{3}$$

2) Battery Degradation Model: We utilize a cycle life model consistent with findings in [6] and [12], to capture the non-linear reality of battery wear. The number of cycles to failure N_{cyc} is modeled as a power-law function of Depth of Discharge (DoD):

$$N_{cyc}(DoD) = A \cdot DoD^k \tag{4}$$

Based on curve fitting of Li-ion data, we computed parameters $A \approx 743$ and $k \approx -2.39$. The degradation cost for a specific discharge event is derived as the fraction of cycle life consumed multiplied by the vehicle-specific battery replacement cost V^n_{bat}:

$$C_{\text{deg}}(t) = \sum_{n=1}^{N} \frac{|r^n(t)\Delta t|}{C^n_{cap} \cdot DoD(t)} \cdot \frac{V^n_{bat}}{N_{cyc}(DoD(t))} \tag{5}$$

C. System Constraints

The optimization is subject to the following user satisfaction and physical constraints for each vehicle n:

1) **SoC Dynamics:** The State of Charge (SoC) evolution depends on the charging rate $r^n(t)$, charging efficiency η^n, and the battery's current State of Health (SoH^n):

$$SoC^n(t+1) = SoC^n(t) + \frac{r^n(t) \cdot \Delta t \cdot \eta^n}{C^n_{cap} \cdot SoH^n} \tag{6}$$

2) **Physical Rate Limits:** The charging and discharging rates are bounded by the specific charger and vehicle capacity r^n_{max}:

$$0 \leq r^n(t) \leq r^n_{max} \quad \text{(Charging)} \tag{7}$$

$$-r^n_{max} \leq r^n(t) \leq 0 \quad \text{(Discharging)} \tag{8}$$

3) **Battery Capacity Limits:**

$$SoC_{min} \leq SoC^n(t) \leq SoC_{max} \tag{9}$$

4) **User Satisfaction (Departure Target):**

$$SoC^n(T_{dep}) \geq SoC^n_{target} \tag{10}$$

Where T_{dep} is the user's scheduled departure time and SoC^n_{target} is the user preferred target state of charge at departure.

IV. Proposed Solution and Methodology

The second contribution of this paper required development a new formulation that allows the incorporation of domain-specific constraints into the search method. An evaluation framework was developed to assess the trade-offs between achieving mathematical optimality and heuristic adaptability in real-time control.

A. Baselines

We benchmarked the PR-PSO against three systems: (1) FCFS which serves as a baseline system where EVs start charging at their arrival time; (2) Rolling-Horizon standard PSO which operates as a heuristic method that implements penalty functions which match the design in [12].

B. Proposed Method: Peak-Repair PSO (PR-PSO)

The PR-PSO algorithm solves the "greedy-trader" problem of Standard PSO together with the "myopic" issue which exists the baseline system. The algorithm injects domain knowledge directly into the swarm's position update mechanism via two hard constraints.

1) Laxity-Based Pruning: A dynamic lower bound $r^{lax}_{min}(t)$ for each vehicle is calculated to ensure 100% user satisfaction. This bound represents the minimum power required at time t to ensure the target state of charge at departure SoC^n_{target} remains reachable given the expected remaining dwell time set by the user:

$$r^{lax,n}_{min}(t) = \max\left(-r^n_{max}, \frac{E^n_{needed} - P^{future,n}_{max}}{\Delta t \cdot \eta^n_d}\right) \tag{11}$$

Where $P^{future,n}_{max}$ is the maximum energy that can be physically charged in the remaining future steps, E^n_{needed} is the total energy required to reach the target SoC, and η^n_d is the discharging efficiency. The search space for every particle is strictly clamped to $[r^{lax,n}_{min}, r^n_{max}]$ during updates.

2) Peak Repair Mechanism: The Peak Repair Mechanism is the primary contribution of this work. It effectively transforms the soft economic penalty of monthly demand charge into a hard physical constraint during the search process. The random stochastic particle movements in heuristic approaches, often violates aggregate power limits. This mechanism mathematically projects these infeasible solutions onto the feasible boundary, defined by the historical peak P^{hist}_{peak}, instead of discarding them or applying weak penalties.

For any particle i where the aggregate load $P_{total} = \sum r^n(t)$ exceeds P^{hist}_{peak}, the excess power $\Delta P = P_{total} - P^{hist}_{peak}$ is calculated. To reduce this excess without violating user satisfaction (Eq. 11), the Reducible Power γ^n is defined for each charging vehicle:

$$\gamma^n = \max(0, r^n(t) - r^{lax,n}_{min}(t)) \tag{12}$$

γ^n represents the amount of power that can be temporarily clipped from vehicle n without jeopardizing its ability to reach full charge before departure. The repair operator then distributes this required cut ΔP proportionally among all vehicles based on their available flexibility:

$$r^n_{new}(t) = r^n(t) - \left(\frac{\gamma^n}{\sum_{k\in\mathcal{N}} \gamma^k}\right) \cdot \Delta P \tag{13}$$

This ensures that the aggregate peak constraint is satisfied. Moreover, vehicles with tighter deadlines (low γ^n) are protected from aggressive throttling while vehicles with high flexibility contribute most to peak shaving. The proposed algorithm flowchart is displayed in

Fig. 1. The framework operates on a dual-layer temporal structure. The controller uses the outer loop which monitors physical time step t to track current system conditions which include EV arrivals and SoC and to build dynamic constraints which the system requires for its operational needs. The PR-PSO system operates through its inner loop which implements

its specific operational functions. The procedure establishes feasible solutions through two separate operators which differ from standard heuristics that impose penalties after they finish evaluating constraints. First, the *Laxity-Based Pruning* restricts the particle's search space (Eq. 11) to guarantee that user departure targets are mathematically satisfy-able. The *Peak-Repair* mechanism stops operations before cost evaluation begins; if a particle's total load surpasses its historical maximum, it will be redirected to the appropriate capacity limit based on the flexibility metric γ (Eq. 12-13). The system begins its execution by dispatching the initial interval commands after reaching the optimal schedule point which identifies G_{best} and then moves the projection forward to $t+1$.

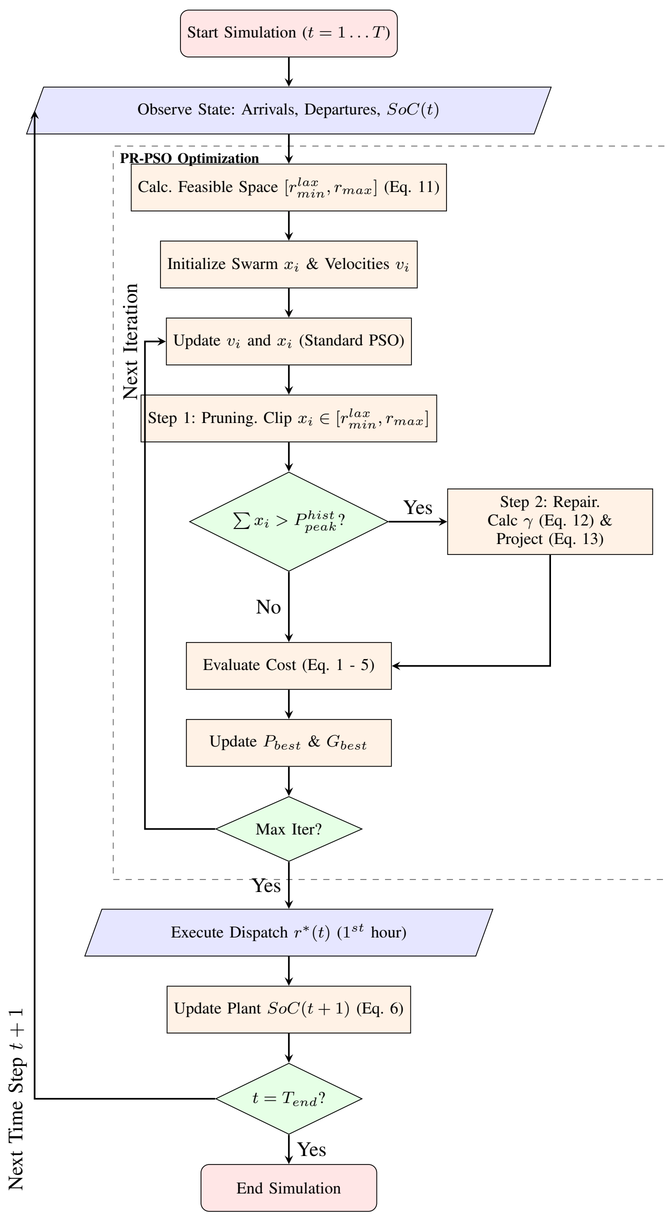

Fig. 1. Computational Flowchart of the PR-PSO Framework. The dashed box indicates the optimization loop performed at every time step t.

V. Results and Discussion

A. Simulation Setup

The developed VPP controller was simulated over a short 7-day period and a longer 30-day period. The fleet composition and simulation parameters are detailed below.

TABLE I
Heterogeneous EV Fleet Specifications

EV Model	Cap. (kWh)	Charge (kW)	V2G (kW)	Class
Tesla Model S	100	11.5	-11.5	Premium
Tesla Model 3	75	11.5	-11.5	Premium
Ford Mustang Mach-E	88	10.5	-9.5	Premium
BMW i3	42	7.4	-5.0	Premium
VW ID.4	82	11.0	-10.0	Mid
Nissan Leaf	62	6.6	-6.0	Mid
Chevrolet Bolt	66	7.2	-7.2	Mid
Hyundai Kona	64	7.2	-6.5	Mid
BYD Atto 3	60	7.0	-6.0	Economy
Renault Zoe	52	7.4	*N/A*	Economy

TABLE II
System Constants and Simulation Parameters

Parameter	Symbol	Value
Infrastructure & Economics		
Demand Charge Rate	R_{demand}	\$15.48 / kW
On-Peak Energy Price	p_{on}	\$0.25 / kWh
Off-Peak Energy Price	p_{off}	\$0.06 / kWh
Charger Efficiency	η	0.95
Number of Chargers	N_{ch}	10
Charging Sessions (7-days)	$N_{session}$	30
Charging Sessions (30-days)	$N_{session}$	120
Battery Degradation Model [6], [12]		
Cycle Life Constant	A	743
Cycle Life Exponent	k	-2.39
Ref. Replacement Cost	V_{bat}	$\approx$ \$150-250/kWh
Constraints		
Min/Max SoC	$SoC_{min/max}$	0.0 / 1.0
Target Departure SoC	SoC_{target}	0.80 - 0.97

B. Data Generation and System State Initialization

The EV arrival and departure sessions were created according to actual charging data distribution from ACN-Data platform [7], [8] to test the algorithms under real-world stochastic conditions. The initial State of Charge ($SoC_{arrival}$) was modeled through a normal distribution that was truncated to show values between 40% and 60% which represent common daily travel energy usage. Users set their departure targets (SoC_{target}) to values that had a uniform distribution between 80% and 97% which showed different degrees of fear about running out of battery power.

The fleet composition shown in Table I was chosen based on market distributions which show 25% of the fleet operating with premium models and 60% with mid-range models and

15% with economy models. The VPP system needs to control assets which have extreme differences in their flexibility capabilities (γ^n).

The system requires an initial value of zero for historical peak power state (P_{peak}^{hist}) at the start of the 30-day billing cycle to achieve proper simulation of rolling-horizon demand charge myopia. The system updates the historical peak state permanently when actual executed aggregate dispatch $\sum r^*(t)$ exceeds P_{peak}^{hist} at each physical time step t. The system uses updated P_{peak}^{hist} state to establish boundary limits which the PR-PSO system maintains during its optimization process.

C. Comparative Performance Analysis

This section presents an analysis of the controllers. The results show average outcomes which were obtained through an 11-run Monte Carlo simulation tests because the system needed to handle unpredictable driving patterns of electric vehicles and the random starting points of particle swarm optimization tests. Their behavior is first examined over a 7-day horizon, and then over a full 30-day billing cycle demonstrating the cumulative impact. The "Horizon Effect" which appears in rolling-horizon optimization exists as the main factor which separates these two groups.

1) Short-Term Analysis (7-Day): Table III provides an overview of the average performance results from the first week. The conventional PSO-based controller succeeded in energy arbitrage optimization during this short time period. The system lacks the ability to predict upcoming monthly peak penalty periods. The system produced demand charge costs which reached an average of \$135.66. This amount almost completely offset the energy profits. Most pricing systems impose demand charge costs on a monthly basis. These costs will not be fully realized until the complete duration of this analysis. The net cost from this period shows that the conventional PSO system costs \$226.25 which is slightly cheaper than the uncontrolled FCFS baseline pricing of \$232.29. The peak demand charges will create stronger negative impacts which will become visible during the extended evaluation period.

The PR-PSO system operates its power grid through its capability to control total power consumption which results in lower estimated demand costs that reach \$87.72. The system achieves operational cost optimization through heuristic methods which result in demand charge decreases that create an estimated Net Total Cost of \$109.83. This cost represents a 51% decrease from the PSO-based traditional method while showing superior performance to the FCFS system during initial periods.

TABLE III
7-Day Cost Analysis (Short-Term)

Controller	V2G Revenue (\$)	Est. Demand Charge (\$)	Op. Cost (\$)	Est. Net Cost (\$)
FCFS	0.00	120.45 ± 21.48	111.84 ± 10.68	232.29 ± 24.85
PSO-Std.	42.58 ± 8.20	135.66 ± 29.90	133.17 ± 15.00	226.25 ± 31.38
PR-PSO (Prop.)	**38.79 ± 7.66**	**87.72 ± 14.20**	**60.89 ± 7.00**	**109.83 ± 17.54**

2) Long-Term Analysis (30-Day): The simulation was then conducted for a complete month and the outcomes appeared in Table IV. The "Myopia" effect becomes punishing here. The conventional PSO-based controller creates a high peak which results in an average Demand Charge of \$656.84 during aggressive V2G services. The accumulated V2G profits cannot cover the penalty because this cost dominates the cost structure. The Net Total Cost of \$1013.31 provides no better results than the basic FCFS method which costs \$1014.13.

The PR-PSO, by actively tracking and reducing the peak throughout the month, achieved optimal results by successfully balancing operational costs and V2G revenues. The system achieved total costs of \$606.68 which marked a 40% cost decrease when compared to both the uncontrolled FCFS charging method and the standard PSO base system. This study demonstrates that demand-charge sensitive VPPs benefit more from constraint-aware heuristics than they do from standard rolling-horizon algorithms which cannot remember peak operational states.

TABLE IV
30-Day Cost Analysis (Long-Term)

Controller	V2G Revenue (\$)	Demand Charge (\$)	Op. Cost (\$)	Net Total Cost (\$)
FCFS	0.00	555.31 ± 82.23	458.82 ± 22.43	1014.13 ± 87.38
PSO-Std.	180.76 ± 16.30	656.84 ± 97.53	537.23 ± 34.21	1013.31 ± 83.48
PR-PSO (Prop.)	**160.07 ± 12.79**	**530.15 ± 74.06**	**236.60 ± 15.99**	**606.68 ± 71.00**

3) Analysis of Peak Power Levels: Research demonstrates that standard heuristic methods exhibited unstable performance during simulation tests which extended over extended periods. The Standard PSO suffers a severe rebound effect, with its average peak surging from 37.6 kW (7-day) to 42.4 kW (30-day). The unrestricted algorithms execute energy arbitrage activities because they need to manage charging operations which automatically lead to multiple grid capacity violations that result in expensive demand charges.

The proposed PR-PSO system effectively controls system volatility because it establishes control mechanisms for this unpredictable behavior. The system reached a 30-day peak of 34.3 kW which exceeded the 7-day measurement of 24.3 kW but remained 19 percent below the Standard PSO benchmark. The PR-PSO repair system prevented the worst-case demand charge penalty which single extreme usage days establish while it completed all energy requirements. V2G participation did not affect the PR-PSO peak because it achieved 34.3 kW which stayed below the FCFS baseline of 35.9 kW showing that the system can deliver grid services without generating harmful tariff penalties.

D. Impact of Fleet Diversity

The simulations established that the different assets operated through a distinct labor distribution system. High-capacity bidirectional models like Tesla Model S and VW ID.4 delivered most of the V2G energy services because these models had high flexibility margins which combined with their quick

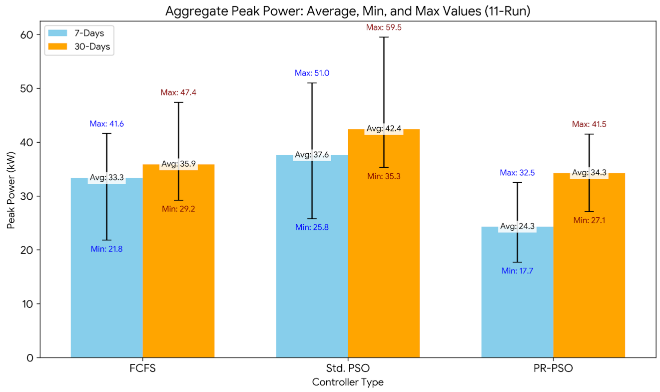

Fig. 2. Aggregate Peak Power Comparison of Impact of the Proposed Control Strategy and Simulation Horizon.

discharge capabilities. The economy models which included Renault Zoe functioned mainly as one-way power sources which helped them reach their required departure time. The PR-PSO system accomplished successful integration between different technical requirements which enabled it to achieve maximum value from flexible resources while maintaining stable peak demand levels.

VI. Conclusion

The research established a VPP orchestration framework which operates with multiple electric vehicle types to show that rolling-horizon MILP fails to handle peak shaving during periods when demand charges constitute the main cost structure. The PR-PSO algorithm used domain-specific repair operators to handle different electric vehicle requirements which resulted in total cost savings exceeding 48

The PR-PSO algorithm will be tested against modern systems which include Deep Reinforcement Learning (DRL) and hybrid meta-heuristic methods in future studies. Future research should include uncertainty quantification and sensitivity analyses to assess system performance during forecast errors from load predictions and unpredictable electric vehicle activities and changes in tariff rates. The framework will gain better realism through the addition of detailed battery degradation simulations which consider temperature effects and C-rate and calendar aging and through the creation of a Multi-Objective Optimization framework which enables Pareto-optimal management of operational costs and battery performance and power grid reliability.

VII. Acknowledgment

The authors acknowledge the support provided by King Fahd University of Petroleum & Minerals (KFUPM) in conducting this research.

References

[1] D. Zheng, L. Liu, G. Tang, et al., "Cost-efficient power orchestration in electric vehicle-integrated vpp using lightweight multi-agent reinforcement learning," *IEEE Transactions on Intelligent Transportation Systems*, 2025.

[2] J. Dong, A. Yassine, A. Armitage, and M. S. Hossain, "Multi-agent reinforcement learning for intelligent v2g integration in future transportation systems," *IEEE Transactions on Intelligent Transportation Systems*, vol. 24, no. 12, pp. 15 974-15 983, 2023.

[3] S. Zhao, X. Lin, and M. Chen, "Peak-minimizing online ev charging: Price-of-uncertainty and algorithm robustification," in *Proceedings of the IEEE INFOCOM*, 2015, pp. 2335-2343.

[4] L. Zhang and Y. Li, "Optimal management for parking-lot electric vehicle charging by two-stage approximate dynamic programming," *IEEE Transactions on Smart Grid*, vol. 8, no. 4, pp. 1722-1730, 2017.

[5] J. Sales-Ortiz and O. Ardakanian, "Efficient trading of aggregate bidirectional ev charging flexibility with reinforcement learning," in *Proceedings of the 15th ACM International Conference on Future Sustainable Energy Systems*, 2024, pp. 134-146.

[6] D. Zheng, L. Liu, G. Tang, Y. Wang, and W. Li, "Power demand reshaping using energy storage for distributed edge clouds," *IEEE Transactions on Parallel and Distributed Systems*, vol. 35, no. 2, pp. 362-376, 2024.

[7] Z. J. Lee, T. Li, and S. H. Low, "Acn-data: Analysis and applications of an open ev charging dataset," in *Proceedings of the 10th ACM International Conference on Future Energy Systems*, 2019, pp. 139-149.

[8] T. Li, *Acn-data-static*, https://github.com/tongxin-li/ACN-Data-Static, Accessed: 2025-09-12, 2023.

[9] Y. Zhang, Q. Yang, D. An, D. Li, and Z. Wu, "Multistep multiagent reinforcement learning for optimal energy schedule strategy of charging stations in smart grid," *IEEE Transactions on Cybernetics*, vol. 53, no. 7, pp. 4292-4305, 2022.

[10] A. Wickramasinghe et al., "A Multi-Objective Framework for EV Scheduling: Balancing Profit and Longevity under Dynamic Operating Envelopes," *IEEE IAS Annual Meeting*, 2025.

[11] S. Rahman et al., "On Efficient Operation of a V2G-Enabled Virtual Power Plant: When Solar Power Meets Bidirectional Electric Vehicle Charging," *ACM e-Energy*, 2021.

[12] R. Khezri, D. Steen, E. Wikner, and L. A. Tuan, "Optimal V2G Scheduling of an EV With Calendar and Cycle Aging of Battery: An MILP Approach," *IEEE Trans. Transp. Electrif.*, vol. 10, no. 4, 2024.

[13] K. Park and I. Moon, "Multi-agent deep reinforcement learning approach for EV charging scheduling in a smart grid," *Applied Energy*, vol. 328, 2022.

[14] K. P. Joshua et al., "Optimized Scheduling of Electric Vehicles Charging in Smart Grid using Deep Learning," *IEEE ICOECA*, 2024.

[15] A. Lilhore et al., "Smart Charge Scheduling of EVs based on User Behaviour Predicted using Machine Learning," *IEEE ECCE-Asia*, 2025.

[16] M. M. Rahman et al., "Scheduling of Electric Vehicle Charging in a Solar-Wind Powered Microgrid Using Machine Learning," *IEEE WIECON-ECE*, 2024.

[17] M.-T. Kuo, "Multi-objective Scheduling of Thermal Generation Units Considering Renewable Energy Intermittency and Electric Vehicle Load Impacts," *IEEE IAS Annual Meeting*, 2025.

[18] S. Heinen, A. Botha, D. Head, R. Parker, and P. Richards, "Customer-centric electric vehicle orchestration in New Zealand: How residential smart charging can deliver affordability and customer satisfaction," *IEEE Power and Energy Magazine*, vol. 21, no. 6, pp. 38-44, 2023.

[19] A. Muqbel, A. T. Al-Awami, and M. Parvania, "Optimal planning of distributed battery energy storage systems in unbalanced distribution networks," *IEEE Systems Journal*, vol. 16, no. 1, pp. 1194-1205, 2022.

[20] X. Wang, Y. Deng, Y. Liu, G. Lian, and H. Jia, "Optimal scheduling strategy of electric vehicles integrated virtual power plant based on improved SAO algorithm," in *2025 6th International Conference on Advanced Electrical and Energy Systems (AEES)*, 2025, pp. 521-526.

[21] C. B. Saner, J. Saha, A. Sharma, and D. Srinivasan, "Heuristic methods for EV charging scheduling in fast charging stations with modular architecture: A comparative analysis," in *2023 IEEE PES 15th Asia-Pacific Power and Energy Engineering Conference (APPEEC)*, 2023, pp. 1-6.

[22] M. I. Hossain, A. T. Al-Awami, and M. A. Abido, "A proportional and weight based decentralized charge controller of electric vehicles for the improvement of local voltage profile," *IEEE Access*, vol. 12, pp. 79699-79712, 2024.

[23] K. M. S. Y. Konara and M. L. Kolhe, "Charging coordination of opportunistic EV users at fast charging station with adaptive charging," in *2021 IEEE Transportation Electrification Conference (ITEC-India)*, 2021, pp. 1-6.